DESIGN OF DUAL-MODE DUAL-BAND PHOTONIC CRYSTAL BANDPASS FILTERS FOR TERAHERTZ COMMUNICATION APPLICATIONS

Ozgur Onder Karakilinc[1] and Mehmet Salih Dinleyici[2]
[1] Department of Electrical and Electronics Engineering, Pamukkale University, 20070 Denizli, Turkey; Corresponding author: okarakilinc@pau.edu.tr
[2] Department of Electrical and Electronics Engineering, Izmir Institute of Technology, 35437 Urla, Izmir, Turkey

Received 30 January 2015

ABSTRACT: *In this study, Photonic Crystal (PhC) dual-mode dual-band bandpass filter is designed and its transmission characteristics are investigated for various configurations. PhC resonator structure is formed by a point defect microcavity that is equipped with one large and three smaller auxiliary perturbation rods. Degenerate modes at each band may also be excited by changing the structure properties of the perturbation. Plane wave expansion method and Finite Difference Time-Domain method are used to analyze the device characteristics. Proposed dual-band dual-mode PhC filter structure can effectively be used for terahertz communication applications.* © 2015 Wiley Periodicals, Inc. Microwave Opt Technol Lett 57:1806–1810, 2015; View this article online at wileyonlinelibrary.com. DOI 10.1002/mop.29196

Key words: *degenerate mode; dual band; dual mode; filter; photonic crystal*

1. INTRODUCTION

Photonic crystals (PhCs) are artificial materials which include a periodic arrangement of dielectric medium and display photonic band gaps depending on their geometry and refractive index profiles. Because of the unique properties on the light guidance, PhCs have become as indispensable tool for light wave manipulation. Several functions like filters, couplers, and multiplexers have already been designed using localized defect modes in PhC [1]. Yet, the need for high speed and high data rate communication systems leads to an increased attention to terahertz (THz) frequencies [2–4]. The micrometers order lattice constant of PhC is very convenient for conventional manufacturing methods and applicable for applications in THz range [5]. Therefore, intense research force has been dedicated to the PhC structures that exhibit various functions necessary in that range [5–7]. Along with the progress in THz communication technologies, filters for multiple frequency bands are highly needed for spectral management in systems with compact design [8]. In this article, dual-mode dual-band PhC bandpass filter is proposed and its transmission characteristics are investigated for various configurations. Degenerate modes of PhC microcavity constructed by a point defect placed at the corner of the line defect waveguide shown in Figure 1 can be splitted by modifying the auxiliary perturbation rods. Exploiting degenerate mode splitting in PhC cavity, single band filter characteristics have been obtained by recent studies [9,10]. Deviating from that studies, in this work, we propose PhC compact bandpass filter exhibiting dual-mode dual-band characteristic. Plane wave expansion method (Mpb) and Finite Difference Time-Domain method (Meep), which are developed by Massachusetts Institute of Technology (MIT) photonic research group, are used to analyze the device characteristics [11].

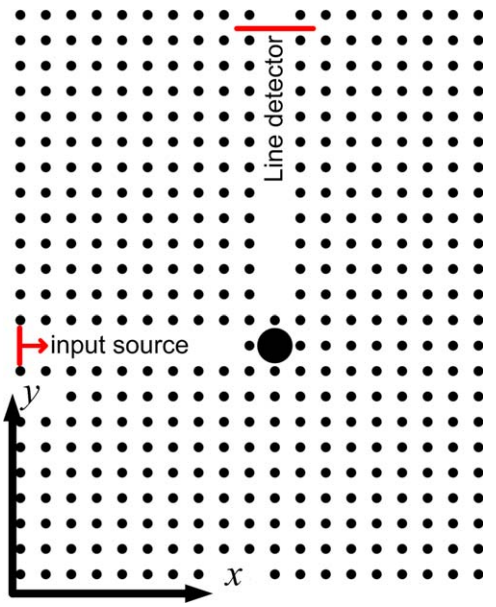

Figure 1 2D PhC structure. [Color figure can be viewed in the online issue, which is available at wileyonlinelibrary.com]

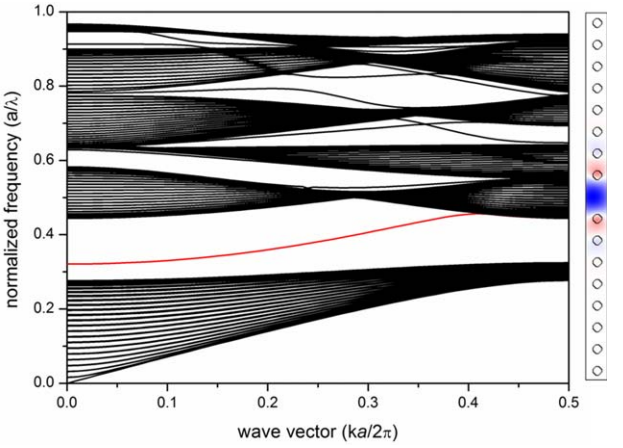

Figure 2 TE (TM, according to Meep) band structure of square PhC with a line defect waveguide and propagated mode profile. [Color figure can be viewed in the online issue, which is available at wileyonlinelibrary.com]

2. PROPOSED PhC MICROCAVITY STRUCTURE

In this study, two-dimensional (2D) square lattice PhC structure with alumina rods in air substrate is considered. As simulation geometry depicted in Figure 1, there is a line defect PhC waveguide with a microcavity having radius r_d that is placed at the bend. PhC dimensions are $25a \times 25a$ along the x and y directions of 2D PhC. The lattice constant "a" is in unit of μm. If the normalized values are used, then all the values in the simulation are normalized with μm and frequency is also normalized to a/λ. All other lengths are expressed in terms of "a" that is set to 400 μm which is very convenient for fabrication [5,12].

The radius of the rods is chosen $0.2a$ and the dielectric constant of alumina is 8.9 (ε). Propagating modes are obtained from the band diagram of line defect PhC as shown in Figure 2 with a red line. Fourier transformed propagated mode profile is computed by MATLAB and applied to the input of waveguide as a plane wave source. Thus, single guided mode (eigenmode) excitation is guaranteed. The transmitted mode fields are detected with a line detector at the output. Throughout the simulations,

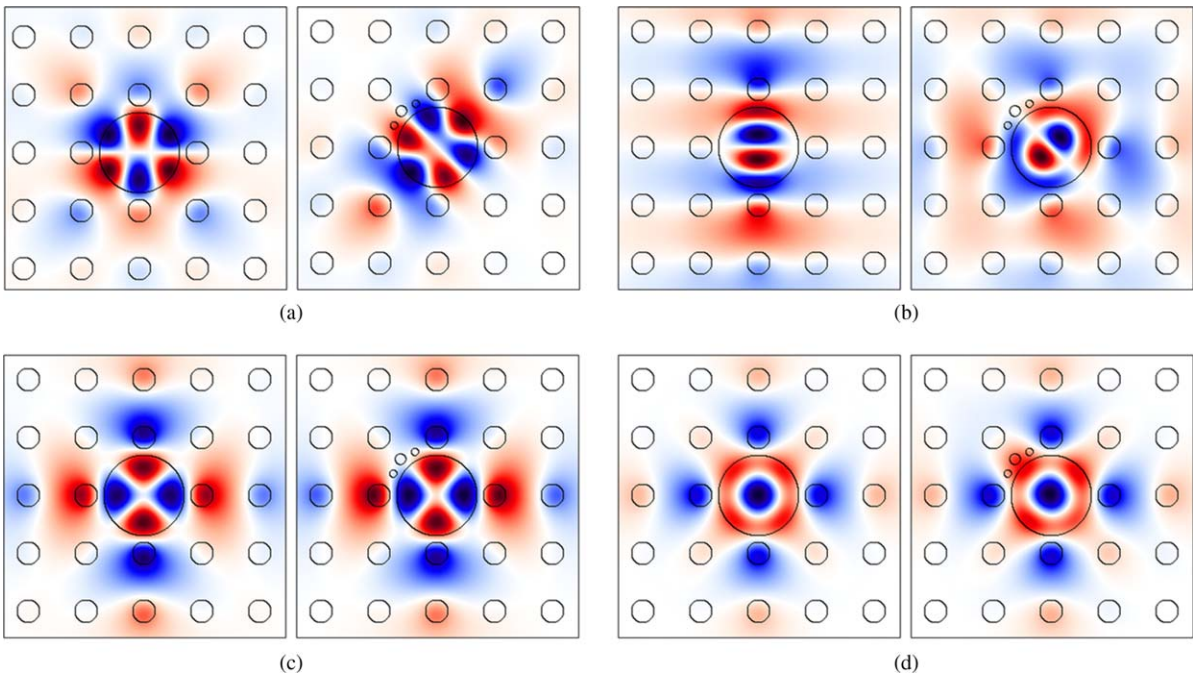

Figure 3 Doubly degenerate (left) and coupled (right) (a) hexapole and (b) dipole modes for 0.29 THz and 0.324 THz, respectively. Non-degenerate (left) and coupled (right) (c) quadrupole and (d) monopole mode for 0.261 THz and 0.264 THz, respectively. [Color figure can be viewed in the online issue, which is available at wileyonlinelibrary.com]

the field is assumed as TE polarized (TM, according to Meep) where the electric field vector is perpendicular to the plane of PhC.

PhC microcavity resonator in this study has C_{4v} symmetry where this structure does not change by 90° rotation. Hence, the cavity modes can be classified as doubly degenerate and nondegenerate in accordance with the symmetry properties. The modes are called nondegenerate if their shapes are invariant under the rotation operator [13]. There are four modes revealed in the PhC microcavity. The two modes are doubly degenerate and the other two are nondegenerate if the radius of microcavity rod is about $0.7a$ [1]. Doubly degenerate hexapole and dipole resonance modes at the frequency of the lower band (0.29 THz) and the upper band (0.324 THz) are shown in Figure 3(a) and quality factor, Q of the microcavity is calculated as 0.3×10^6 and 0.6×10^6, respectively. To excite the degenerate modes in each band simultaneously, a novel perturbation structure is needed and investigated in this study. There are three small perturbation rods at upper left corner of the microcavity. Their names are r_{pmid} and r_p (Fig. 4). Apart from the other perturbation rods, the middle rod has different radius. The refractive index of all perturbation rods is the same as the PhC rods. Exact position of r_{pmid} and r_p are (0.625, 0.625), (−0.375, 0.75), (−0.75, 0.375) points with respect to the center of microcavity rod r_d, (0, 0) in (x, y) plane. The degenerate modes appear by applying the perturbation rods configuration as seen in Figures 3(a) and 3(b). The quality factor of coupled hexapole and dipole modes can be calculated as 1.6×10^6 for 0.29 THz and 0.15×10^6 for 0.324 THz with perturbation $r_p = 0.07a$, $r_{pmid} = 0.1a$. Besides, field distributions of nondegenerate quadrupole and monopole modes persist with the perturbation in Figures 3(c) and 3(d).

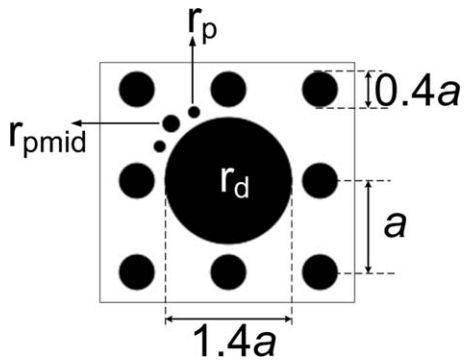

Figure 4 Dual-mode dual-band microcavity

3. DUAL-BAND FILTER CHARACTERISTICS

The filter characteristics are obtained for various perturbation configurations as shown in the Figures 5(a)–5(g). There is no transmission in the line defect waveguide when using the microcavity without perturbation rods as depicted in Figure 5(a). According to Figure 5(b), the transmission spectrum is dramatically changed by introducing a rod $r_{pmid} = 0.07a$ at the upper left corner of microcavity and between two PhC rods. The band at the frequency of 0.29 THz, which is called lower band, is transmitting, but the degenerate modes are splitted as two peaks. Meanwhile, the transmissivity of upper band, at the frequency of 0.324 is increased, but the reflection level is more than −5 dB. The transmission begins at the upper band with the larger value of r_{pmid} as $0.1a$; however, the degenerate modes in the lower band are overcoupled which means the band is deformed. A degenerate mode in the upper band is not excited in this case as seen in Figure 5(c). If only r_p perturbation is applied as in Figure 5(d), the lower band is turned to transmit; however, the upper band transmission remains at the level of −5 dB. Similarly to Figure 5(c), transmission of the upper band and mode splitting can be seen in Figure 5(e) using the larger value of $r_p = 0.1$. By proposing the novel perturbation structure as seen

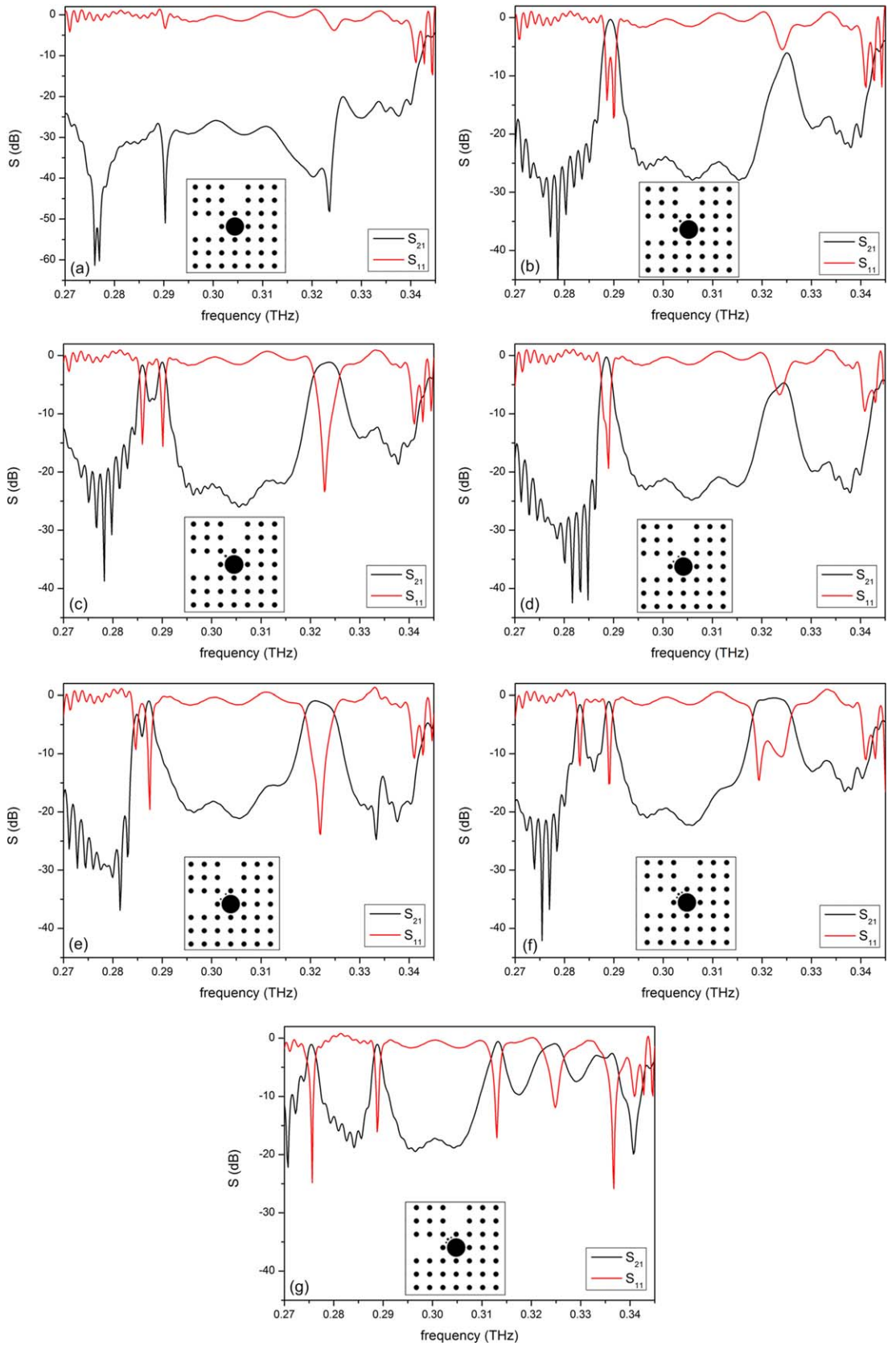

Figure 5 (a) Transmission and reflection spectrum of microcavity with $r_p = 0$ and $r_{pmid} = 0$ (b) $r_p = 0$ and r_{pmid}=0.07a (c) $r_p = 0$ and $r_{pmid} = 0.1a$ (d) $r_p = 0.07a$ and $r_{pmid} = 0$ (e) $r_p = 0.1a$ and $r_{pmid} = 0$ (f) $r_p = 0.07a$ and $r_{pmid} = 0.1a$ (g) $r_p = 0.07a$ and $r_{pmid} = 0.15a$. [Color figure can be viewed in the online issue, which is available at wileyonlinelibrary.com]

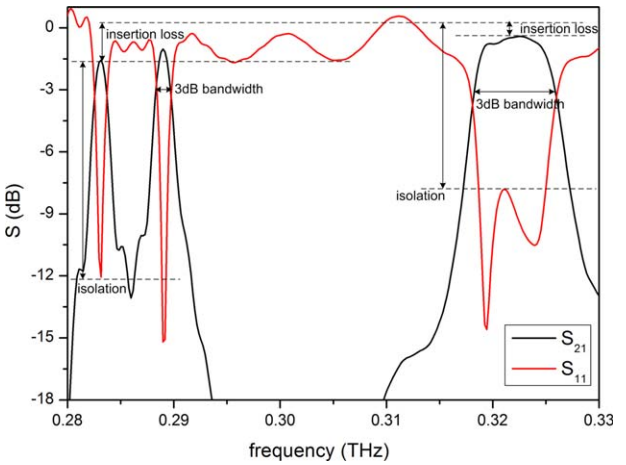

Figure 6 Transmission parameters of the lower and upper band with $r_p = 0.07a$ and $r_{pmid} = 0.1a$. [Color figure can be viewed in the online issue, which is available at wileyonlinelibrary.com]

in Figure 5(f), dual-mode dual-band bandpass filter is obtained by splitting degenerate modes at the both bands. In the last configuration in Figure 5(f), the mode in the upper band is splitted using the perturbation of $r_p = 0.07a$ and $r_{pmid} = 0.1a$. Degenerate modes in the lower band as well as the upper band are overcoupled with a further increase of r_{pmid} as presented in Figure 5(g). According to the simulation results, the isolation is higher than 10 dB and the insertion losses are 1.55 and 1.02 dB as shown in Figure 6. Three-decibel bandwidth is also 0.0011 THz and 0.0014 THz for the left and right modes at lower band, respectively. In contrast to the lower band, the upper band presents larger bandpass filter characteristics with the isolation is higher than 7 dB and the insertion losses is 0.41 dB and 3-dB bandwidth is 0.0075 THz. The upper band exhibits better flat spectral characteristic than the lower band. Fractional bandwidth ($\Delta f/f$) is calculated as % 0.3 and % 0.4 for each mode of the lower band and % 2.3 for the upper band. Fractional bandwidth can be tuned by perturbation rods.

4. OPTIMUM PARAMETERS FOR DUAL-MODE DUAL-BAND FILTER

Various forms of the PhC microcavity structures have been investigated by changing radius of the perturbation rods, r_{pmid} $0.03a$ to $0.15a$ while the r_p is set to $0.05a$. The lower band at frequency 0.29 THz is excited before the upper band at frequency 0.324 THz. The critical coupling value of r_{pmid} is $0.03a$ and $0.10a$ for the lower band and the upper bands, respectively. At the values $0.10a$ of the r_{pmid}, then the upper band is to split as shown in Figure 7(a). Adjusting the middle perturbation rods radius r_{pmid} as $0.11a$, both bands can be simultaneously excited. Spectral shift between the degenerate mode frequencies in each band is increased by r_{pmid}. Transmission coefficient (S_{21}) and bandwidth of the both bands are also increased by r_{pmid}. But for the larger values of r_{pmid}, the upper band is over coupled because of the decreasing S_{21} as seen in Figure 7(b). Besides,

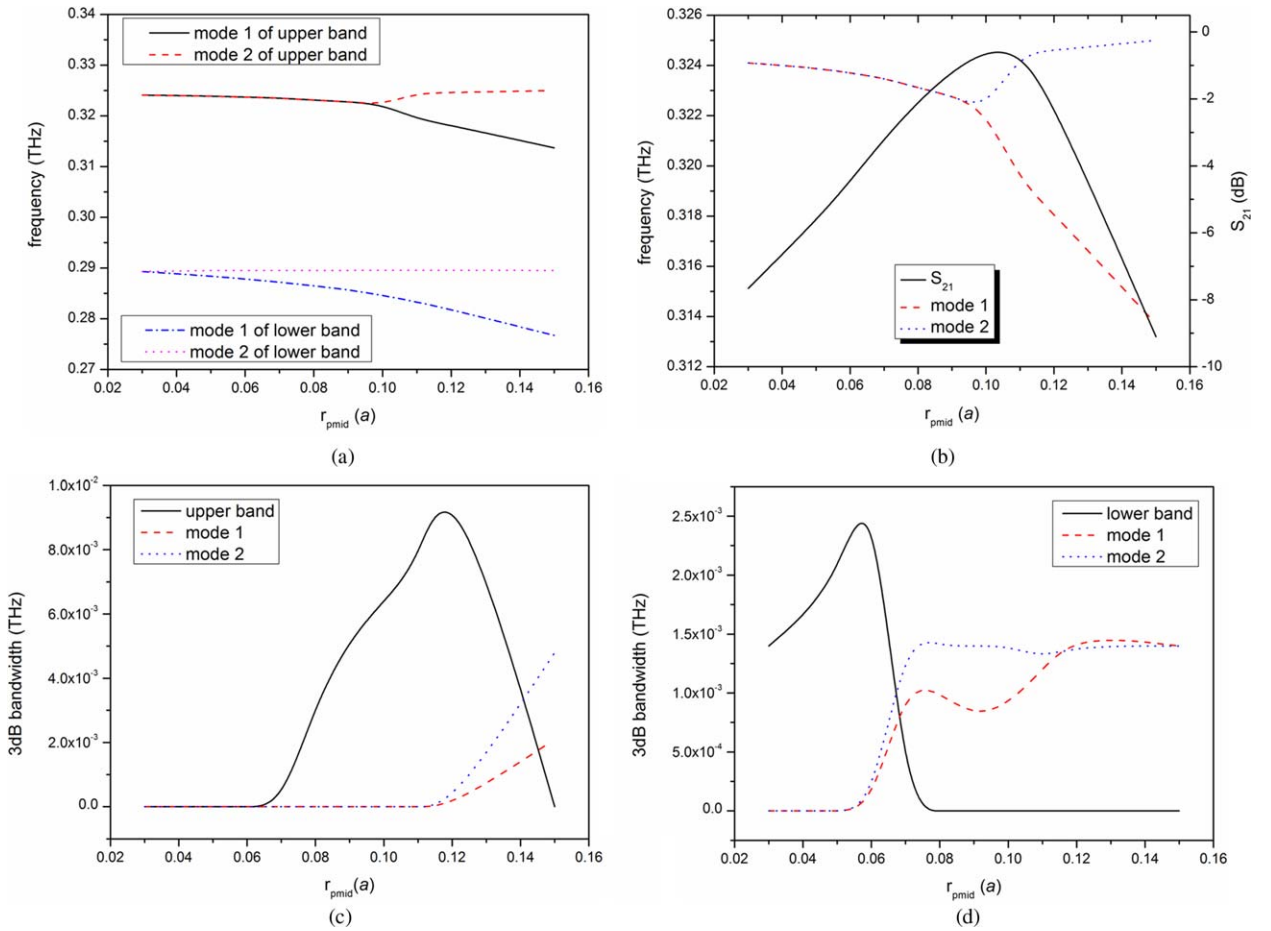

Figure 7 Band splitting properties for r_{pmid} variation (r_p is set to $0.05a$). [Color figure can be viewed in the online issue, which is available at wileyonlinelibrary.com]

when the splitting of modes is increased by r_{pmid}, the bandwidth of modes is increased as depicted in Figures 7(c) and 7(d). Additionally, resonance mode frequency can be tuned with exploiting nonlinearity in PhC cavity. If refractive index of the microcavity rod is increased about %1, the band frequency shifts about 0.003 THz to lower frequency part of the spectrum. Apart from the index change of microcavity rods, the transmission spectrum is not affected by the index variation of perturbation rods. The modes can be easily tuned by perturbation rod structure and/or nonlinear index variation of microcavity rod.

5. CONCLUSION

In this article, we have proposed PhC microcavity structures having perturbation rods that show dual-mode, dual-band filter characteristics with narrow bands, high isolation, low insertion loss, and high quality. The degenerate modes at each band can be activated concurrently with the perturbation rods with $r_p = 0.05$ and $r_{pmid} = 0.11$. The upper band presents flat spectral characteristics as bandwidth is 0.0076 THz with fractional bandwidth % 2.3 at 0.322 THz. The lower band becomes overcoupled with the larger value of r_{pmid}. However, it can be used as a narrow band filter with the bandwidth of 0.0012 THz and 0.0014 THz and fractional bandwidth of % 0.4 for each mode of 0.283 THz and 0.289 THz, respectively. Although the transmission spectrum is dramatically affected by changing the perturbation rod structure (dimension), changing the refractive index of the perturbation rods does not produce similar effects. Additionally, the band frequency is shifted about 0.003 THz to lower frequency part of the spectrum by the refractive index of the microcavity rod is increased about %1. This study may contribute to the development of functional devices for wireless communication application at THz range.

REFERENCES

1. R.D. Meade, J.D. Joannopoulos, S.G Johnson, and J.N Winn, Photonic crystals: Molding the flow of light, 2nd ed., Princeton University Press, New Jersey, 2008.
2. T. Kleine-Ostmann and T. Nagatsuma, A review on terahertz communications research, J Infrared Millimeter Terahertz Waves 32 (2011), 143–171.
3. H. Shirai, K. Ishii, H. Miyagawa, S. Koshiba, S. Nakanishi, and N. Tsurumachi, Efficient terahertz emission, detection, and ultrafast switching using one-dimensional photonic crystal microcavity, J Opt Soc Am B 31 (2014), 1393–1401.
4. Z. Wu, A. Young, M. Gehm, and H. Xin, Investigation of several terahertz electromagnetic band gap structures, Microwave Opt Technol Lett 52 (2010), 678–686.
5. S. Kirihara, Fabrication of photonic crystal cavities for terahertz wave resonations, Nanofabrication, 2011.
6. D. Yang, T. Li, L. Rao, S. Xia, and L. Zhang, Terahertz functional devices based on photonic crystal and surface plasmon polaritons, Terahertz Sci Technol 5 (2012), 131–143.
7. L. Rao, D. Yang, and Z. Hong, Guiding terahertz wave within a line defect of photonic crystal slab, Microwave Opt Technol Lett 54 (2012), 2856–2858.
8. Q. Huang, X. Zhang, J. Xia, and J. Yu, Dual-band optical filter based on a single microdisk resonator, Opt Lett 36 (2011), 4494–6.
9. C. Chun-ping, T. Anada, S. Greedy, T.M. Benson, and P. Sewell, A novel photonic crystal band-pass filter using degenerate modes of a point-defect microcavity for terahertz communication, Microwave Opt Technol Lett 56 (2014), 792–797.
10. A. Daraei and F. Khozeymeh, Investigation on mode splitting and degeneracy in the L3 photonic crystal nanocavity via unsymmetrical displacement of air-holes, Int J Eng Sci 2 (2013), 146–150.
11. A.F. Oskooi, D. Roundy, M. Ibanescu, P. Bermel, J.D. Joannopoulos, and S.G. Johnson, Meep: A flexible free-software package for electromagnetic simulations by the FDTD method, Comput Phys Commun 181 (2010), 687–702.
12. M.J. Fitch and R. Osiander, Terahertz waves for communications and sensing, Johns Hopkins APL Tech Dig 25 (2004).
13. S. Kim and Y. Lee, Symmetry relations of two-dimensional photonic crystal cavity modes, IEEE Int J Quantum Electron 39 (2003), 1081–1085.

A DUAL-BAND COMPACT PRINTED MONOPOLE ANTENNA USING MULTIPLE RECTANGLE-SHAPED DEFECTED GROUND STRUCTURES AND CROSS-SHAPED FEED LINE

Sanjeev Kumar and Raghuvir Tomar
Department of Electronics and Communication Engineering, The LNM Institute of Information Technology, Jaipur 302031, India; Corresponding author: rtomar@lnmiit.ac.in, tomarlnmiit@gmx.com

Received 30 January 2015

ABSTRACT: *A compact printed monopole antenna with dual-band operation at 1.8 GHz (GSM Band) and 5.2 GHz (Wi-Fi Band) is presented. The antenna consists of a modified U-shaped radiating patch with a triple rectangular defect in the ground plane. The antenna is fed by a cross-shaped feed line, which helps in realizing the dual-band operation. The antenna has been designed using RO4350 substrate. The design size achieved is 19 × 28 mm^2. An impedance bandwidth of about 32% at 1.8 GHz and about 29% at 5.2 GHz for 10 dB return loss has been achieved. A size reduction of about 12% in comparison with a similar antenna without defected ground structures has been achieved. The proposed antenna has been fabricated and tested, and a good agreement between simulated and measured results is seen. Acceptable E-plane and H-plane radiation patterns have been observed through simulations, and a peak antenna gain of about 2.8 dBi has been achieved.* © 2015 Wiley Periodicals, Inc. Microwave Opt Technol Lett 57:1810–1813, 2015; View this article online at wileyonlinelibrary.com. DOI 10.1002/mop.29195

Key words: *defected ground structure; dual-band; impedance bandwidth; microstrip; Wi-Fi; GSM*

1. INTRODUCTION

Compact dual-band microstrip antennas are much in demand nowadays, as such antennas facilitate integration of different radio modules into the same piece of equipment [1]. The use of defected ground structures (DGSs) is one currently popular method used to reduce the design size of microstrip antennas (e.g., [2–11]). This article proposes a new symmetrical printed monopole antenna using multiple rectangular DGSs, for dual-band operation at GSM and Wi-Fi bands. The presence of the DGS perturbs the current distribution in the ground plane, and thus, modifies the equivalent transmission line parameters over the defected regions [2–4]. Put differently, the DGS uses its slow-wave characteristics to reduce the size of the design. In practical terms, the use of the DGS enhances the antenna bandwidth by an amount that depends on the shapes, the locations, and the dimensions of the defects [5–11].

In the design reported herein, the use of the multiple rectangular-shaped DGSs is made to increase the bandwidth of the antenna, and to reduce the design size. A cross-shaped feed line is used to achieve the dual-band operation. The proposed structure, shown in Figure 1, resonates at 1.8 and 5.2 GHz. The design dimensions have been optimized using the HFSS